Baghdad Science Journal

Volume 22 | Issue 8 Article 7

8-15-2025

Hydrothermal synthesis of high surface area mesoporous silica as an efficient adsorbent for removal of crystal violet dye from aqueous solution

Inaam H. Ali
Department of Chemistry, College of Science for Women, University of Baghdad, Baghdad, Iraq., inaam.mohmmed@gmail.com

Ameera Hassan Hamed
Department of Chemistry, College of Science for Women, University of Baghdad, Baghdad, Iraq., ameerahh-chem@csw.uobaghdad.edu.iq

Ennas Abdul Hussein
Department of Chemistry, College of Science for Women, University of Baghdad, Baghdad, Iraq., enaasak-chem@csw.uobaghdad.edu.iq

Saadiyah A. Dhahir
Department of Chemistry, College of Science for Women, University of Baghdad, Baghdad, Iraq., sadiataher@csw.uobaghdad.edu.iq

How to Cite this Article

Ali, Inaam H.; Hamed, Ameera Hassan; Hussein, Ennas Abdul; and Dhahir, Saadiyah A. (2025) "Hydrothermal synthesis of high surface area mesoporous silica as an efficient adsorbent for removal of crystal violet dye from aqueous solution," *Baghdad Science Journal*: Vol. 22: Iss. 8, Article 7.
DOI: https://doi.org/10.21123/2411-7986.5018

BAGHDAD SCIENCE JOURNAL 2025;22(8):2550–2561

RESEARCH ARTICLE

Hydrothermal Synthesis of High Surface Area Mesoporous Silica as an Efficient Adsorbent for Removal of Crystal Violet Dye From Aqueous Solution

Inaam H. Ali *, Ameera Hassan Hamed, Ennas Abdul Hussein, Saadiyah A. Dhahir

Department of Chemistry, College of Science for Women, University of Baghdad, Baghdad, Iraq

ABSTRACT

In this work, a sample of mesoporous silica (MPS) with a high surface area was prepared by hydrothermal synthesis procedure. To investigate the properties of the prepared sample, it was characterized using different techniques like N_2 Adsorption-desorption, Scanning electron microscopy (SEM), X-ray diffraction (XRD) and Atomic Force microscopy (AFM). In order to evaluate the efficiency of the prepared MPS, adsorption study was carried to examine the ability of MPS to remove crystal violet dye (CV) from aqueous solution. The study was done in different conditions of initial concentration (25–60 mg/L) of dye, dosage of MPS (0.01–0.05 g) and temperature range (293–323 K). The results were applied to three adsorption isotherms which are, Langmuir, Freundlich and Temkin models and gave a very high match with Freundlich equation ($R^2 = 0.9678$). The kinetics of adsorption study was also applied using first order and second order kinetics model in addition to intra particle diffusion model. It reveals that removals of CV dye by MPS is a second order reaction and diffusion step is not the only limiting steps as the linear equation of intraparticle diffusion did not pass through origin. Thermodynamic investigation reveals spontaneous behavior and endothermic nature of adsorption process.

Keywords: Crystal violet, High surface area, Hydrothermal, Mesoporous silica, Sodium silicate

Introduction

Since being found by Mobil scientists in the 1990s, mesoporous silica has attracted a lot of attention by scientific community in many fields, including drug delivery, catalysis, and adsorption and energy storage.[1–4] These materials are widely employed in pharmaceutical administration and adsorption processes due to its surface characteristics, such as significant specific surface area and pore size. In addition, mesoporous silica is now establishing itself as a prominent class of nanomaterials.[5]

Sol-gel, micro-emulsion, and hydrothermal synthesis are three important approaches for producing mesoporous silica. Hydrothermal synthesis tends to be the most efficient as well as easiest of these procedures due to its unique characteristic: it can completely dissolve the precursor, thereby shortening the material reaction time, while also increasing the material's hydrothermal stability.[6] In this method, surfactants are used as a template agent and acid or alkali as a catalyst. After which an inorganic component is gradually added to the combined solution to form a hydrogel that is then placed in the autoclave at high temperature and pressure.[7] As a result, this method has been widely used in the synthesis of mesoporous silica with unique characteristic for environmental applications.[8,9]

Received 11 October 2023; revised 1 June 2024; accepted 3 June 2024.
Available online 15 August 2025

* Corresponding author.
E-mail addresses: inaam.mohmmed@gmail.com (I. H. Ali), ameerahh-chem@csw.uobaghdad.edu.iq (A. H. Hamed), enaasak-chem@csw.uobaghdad.edu.iq (E. A. Hussein), sadiataher@csw.uobaghdad.edu.iq (S. A. Dhahir).

https://doi.org/10.21123/2411-7986.5018

Many kinds of mesoporous materials with diverse structures and pore sizes have been discovered by using different types of surfactants as template. Cationic and nonionic surfactants are most commonly used as the template to form mesoporous materials,[10,11] but only disordered mesoporous materials could be obtained by using anionic surfactants.[12] Zwitterions-surfactant-templated mesoporous silica with highly ordered mesostructured have been rarely prepared.

Huge amounts of dyes are regularly used to color products in several industries, such as printing, papers, textiles, and sand. Some dyes are introduced into the product during the coloring process, and some of them end up in the effluent. There are thousands of synthetic dyes on the market at present. Some of them can be used to color food and beverages while still being healthy for people, but others can be causing harm and possibly hazardous to their health.[13] Ionic dyes tend to be water soluble, which poses potential dangers to both the environment and human health. As a result, several studies have been attracted to the removal of ionic dyes from wastewater.[14–17] A particular kind of these dyes that has an adverse impact on human health is crystal violet. Even at low concentrations, crystal violet (CV) can cause allergies and skin cancer.[18] They are poisonous, mutagenic, and carcinogenic. After ingesting crystal violet by mouth, it is possible to get nausea, vomiting, diarrhea, and gastritis.[19]

Because of its low cost, high efficiency, simple procedure, and simple design, adsorption has become one of the most versatile and widely applied techniques in water treatment technology. Therefore, the objective of the present work was to explore the possibility of removing the synthetic dye CV by a high surface area of MPS and optimizing the best conditions to yield highly efficient adsorption process. The method of preparation the adsorbent was hydrothermal method using a cocamidopropyl betaine a type of zwitterion surfactant as a template and an inexpensive sodium silicate as a precursor of silica.

Materials and methods

Materials

Cocamidopropylbetaine (CAPB) as a zwitterions surfactant (28% in water) was obtained from the state company of plants oil, sodium silicate (water glass, 14% NaOH + 27% SiO_2) was purchased from local market, crystal violet dye (CV) was supplied from (BDH) and sulfuric acid is ACS, reagent with concentration 95%.

Synthesis method

MPS was prepared by dissolving 12 g of CAPB in 150 ml of distilled water, after that (17 ml) of 1M H_2SO_4 was add to the solution with continuous stirring. The sodium silicate (3.5 g) was dissolved in 150 ml of distilled water in a separate container, then placed in a burette, and added onto the acid-surfactant solution drop by drop over duration of three hours to control the pH of the reaction mixture. The final solution was heated for 24 hours at 80 °C in the autoclave until a white precipitate developed at which point it was collected by filtration. The product was washed in water, and the surfactant that was used was removed through four hours of calcinations at 600 °C.[10]

Adsorption method

A 500 mL volumetric flask was used to prepare 1000 mg/L of CV by dissolving 0.5 g of this dye in distilled water to obtain the stock solution. As required for the calibration curve, different concentrations (1–10 mg/L) of the corresponding dye stock solution have been prepared. The absorbance has been measured at the wavelength of 592 nm using a Shimadzu double-beam UV–Vis spectrophotometer.

Batch adsorption studies have been carried out to assess how the system's performance is influenced by a number of variables, such as the temperature, contact time, adsorbent amount, and CV concentration.

The amount adsorbed of CV dye on the mesoporous silica was determined as follow: Eq. (1).

$$q_e = \frac{(C_0 - C_e)\, V}{w} \tag{1}$$

Where V is the volume of solution in liters, C_0 and C_e are the concentrations of CV (mg/L) during the initial and equilibrium adsorption stages respectively, and w is the weight of MPS in grams.

For a 15 mg/L CV concentration, the impact of the adsorbent quantity was investigated using a range of adsorbent amounts (0.01–0.05) g/50 mL of dye. The thermostatic shaker bath's agitation speed was set at 200 rpm for all experiments, and the temperature was maintained at 298 K.

By employing 0.01g of adsorbent in 50 ml of CV solution (15 mg/L) in 250 ml flasks, the influence of contact time on the adsorption process of CV was investigated. 2 mL of sample was poured out every 10 minutes, and the concentration was determined till equilibrium had been established. Adsorption isotherms were studied in the temperature range of 288–318 K by taking a range of concentration

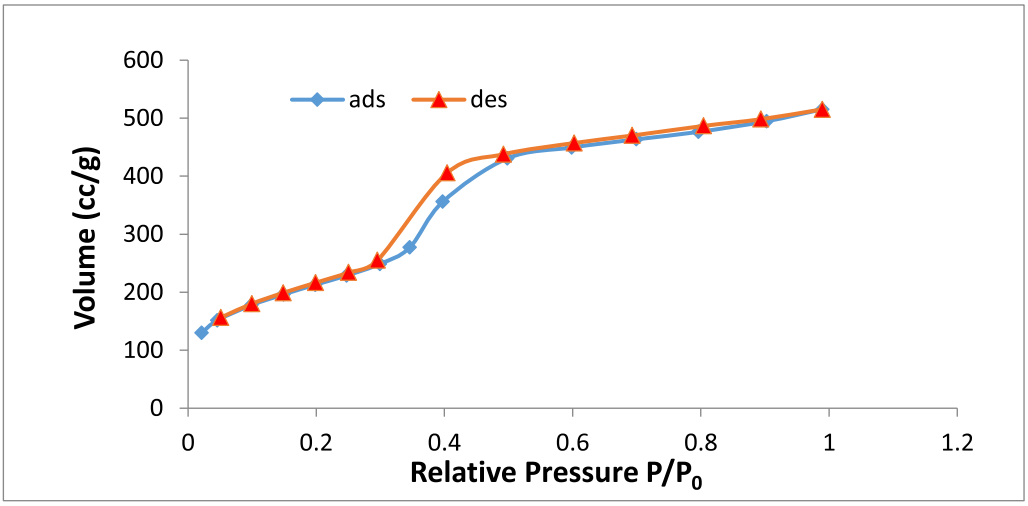

Fig. 1. Adsorption-desorption hysteresis loop for the prepared MPS.

(25–60 mg/L) of dye with constant amount of MPS (0.01g) and a fixed contact time reached to 60 min.

Results and discussion

Characterization of synthesized adsorbent

N_2 adsorption-desorption isotherm

The adsorption-desorption of nitrogen gas at 77 K provides an analysis of surface area, pore volume, pore size, and pore size distribution for MPS prepared in this study. As shown in Fig. 1 as a qualitative analysis the adsorption isotherms for the MPS can be considered type IV according to the common classification of adsorption isotherms and a steep capillary condensation step occurred at a relative pressure (P/P_0) ranging from 0.299 to 0.498. According to the IUPAC classification, the hysteresis loops seen are characteristic for mesoporous materials and match loops of type H1.[20] The BET surface area was found equal to 778.7 m^2/g and the pore volume 8.723 cm^3/g and the pore size 4.09 nm.

Atomic force microscopy (AFM)

The particle size and surface organization of the prepared MPS were evaluated using atomic force microscopy. Fig. 2 displays the surface roughness of the material under investigation. It demonstrates that the average particle size was 76.92 nm, while the diameter of the particles ranged from 20 to 100 nm.

Scanning electron microscopy (SEM)

SEM microscopy is used to identify the size and shape of the prepared MPS. The surface morphology for the prepared sample is shown in Fig. 3 and show rod particle shape with highly dense aggregation. The image displays range of nanoparticles size approximately between (50–85 nm). EDX image shows percentages of silicon and oxygen in the prepared sample which were 52.2% and 47.6% respectively, while disappearance of sodium confirms effective removal of impurities from the sample.[21]

X-Ray diffraction (XRD)

The XRD pattern of the prepared MPS is shown in Fig. 4. Two intense peaks around $2\theta = 0.76$ and 1.46 indexed as (100), (110) reflections were observed which confirmed the characteristic of a two-dimensional (2D) hexagonal (6 mm) structure with spacing of approximately 3.8 nm.[22]

Adsorption of CV dye on prepared sample

Effect of time on adsorption process

Concentrations of 15 mg/L of CV dye were used in this study to investigate the period of time that it takes for the adsorption equilibrium to be attained. Fig. 5 depicts the change of the adsorbed quantity over time, presents the results. It can observe from the figure that two phases appear the first fast and the subsequent slow, until the equilibrium is practically reached after 60 minutes. This is caused by the high initial availability of the adsorbent-free active sites, which decreases as the adsorption proceeds.[23]

Effect of MPS dosage on adsorption process

The effect of MPS dosage on adsorption of CV dye was achieved by determines the quantity of dye adsorbed in mg per weight of MPS in g (0.01–0.05 g). The result was shown in Fig. 6 revealing that the quantity of CV dye adsorbed on MPS is

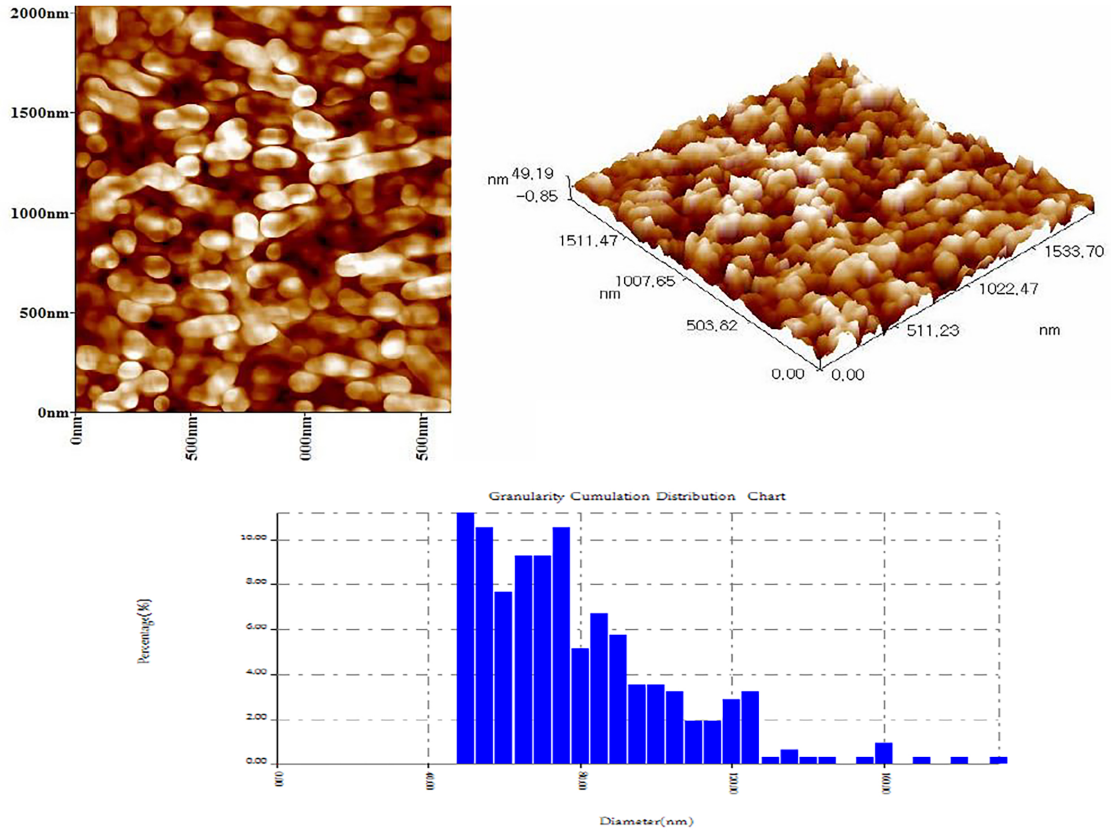

Fig. 2. AFM images and granularity accumulation distribution.

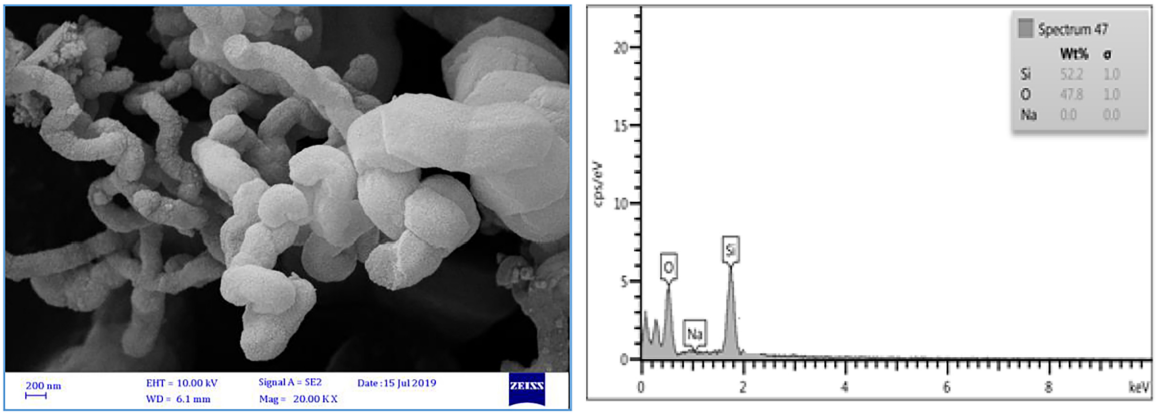

Fig. 3. SEM and EDX images of the prepared MPS

decreases as the dosage increased due to accumulation of adsorbent particles and decreases the ratio of adsorbate/adsorbent quantity where the concentration of dye constant (15 mg/L) with increasing amount of MPS.

Adsorption isotherms of CV-MPS system

Adsorption isotherm is a crucial model for describing adsorption behavior in solid-liquid adsorption systems. The mechanisms of adsorption, the characteristics of the surfaces, and the affinity of the adsorbate for the adsorbent have all been described via isotherms analysis. A range of concentration of CV dye (25–60 mg/L) was used to describe this process by plotting q_e versus C_e using many adsorption models. In this study, three of the most important isotherms were applied to investigate the adsorption phenomena of CV on MPS, there were Langmuir, Freundlich and Temkin isotherms.

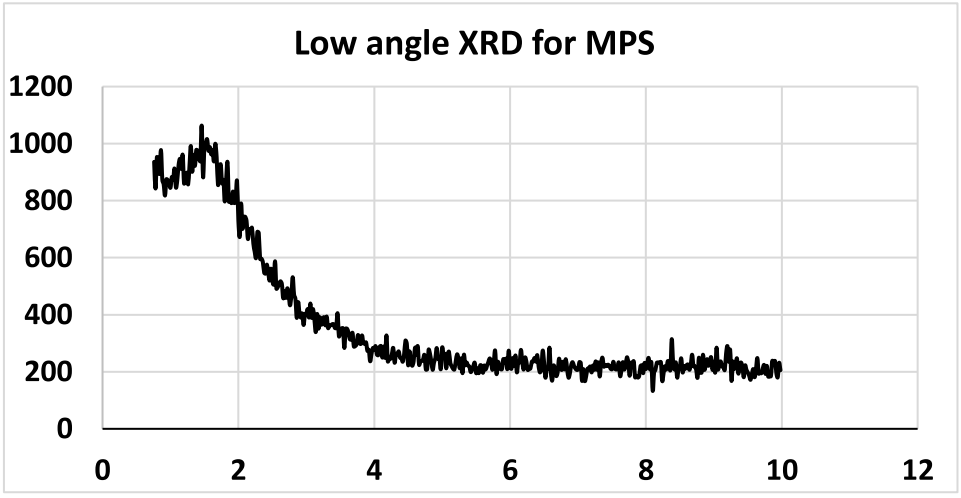

Fig. 4. XRD of the prepared MPS.

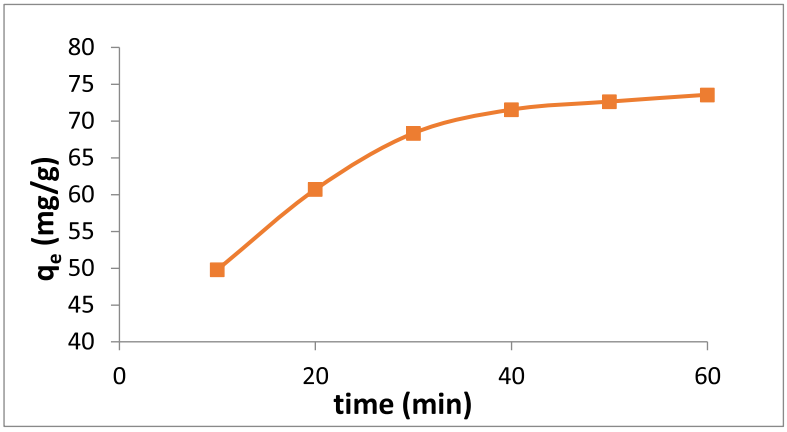

Fig. 5. The effect of time on adsorption process.

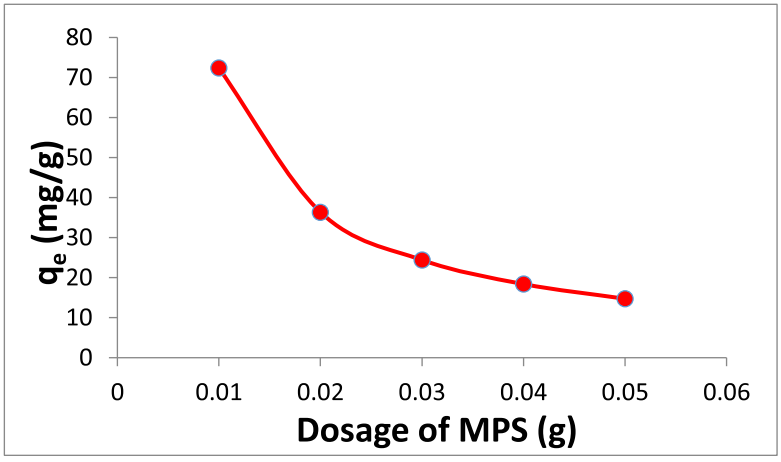

Fig. 6. The amount adsorbed of CV dye affected by MPS dosage.

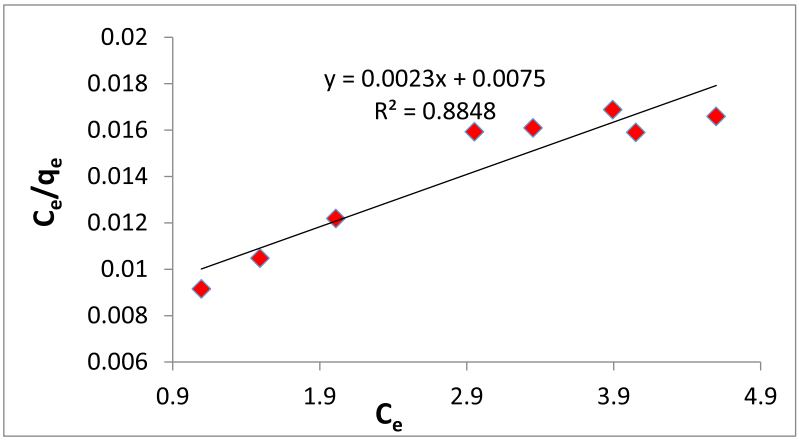

Fig. 7. Linear plot of Langmuir model for CV-MPS adsorption process.

Langmuir model[24] Eq. (2), which was assumed that the surface is homogeneous, adsorption on surface is localized, and each site can accommodate one molecule, was used to describe the equilibrium between the CV dye and MPS, which can be express as follow:

$$\frac{C_e}{q_e} = \frac{1}{K_L.Q^\circ} + \frac{C_e}{Q^\circ} \quad (2)$$

K_L (L/mg) represents the constant of Langmuir, Q° (mg/g) is the maximum adsorption capacity and they were determined by graphing C_e/q_e directly versus C_e, and the slope and intercept values are extracted from straight line equation as shown in Fig. 7.

Another mathematical equation for the adsorption equilibrium between liquid and a solid is called a Freundlich isotherm. Freundlich derived Eq. (3) as an empirical relation to describe the isothermal variation of adsorption of an adsorbate onto the surface of an adsorbent:[25]

$$\ln q_e = \ln K_f + \frac{1}{n} \ln C_e \quad (3)$$

Where K_f (mg/g) and n are Freundlich constants which influenced by the types of materials adsorbed and solids as well as their temperatures. The 1/n quantity obtained from the Freundlich equation can be used to indicate either the extent of curve of the isotherms within the concentration range examined or the linearity of adsorption. Fig. 8 illustrates how the intercept and slope of the estimated line of lnqe against ln C_e obtained the values of K_f and n, respectively.

The Temkin isotherm[26] has a parameter that effectively accounts for interactions between the adsorbent and adsorbate. Temkin isotherm establishes a prediction that the heat of adsorption for every molecule in the layer will decrease linearly rather than logarithmically with coverage by neglecting the comparatively low and high concentration values. A uniform distribution of binding is seen throughout the equation's derivation by plotting the quantity adsorbed q_e versus lnC_e then determining the constants from the slope and intercept. The following Eq. (4) represents the Temkin model in its linear form:

$$q_e = B \ln K_T + B \ln C_e \quad (4)$$

K_T = equilibrium binding constant of Timken isotherm (L/g).

B is a Temkin constant which has to do with the heat of adsorption. Its definition is given by the formula B = RT/b, where b is the Temkin isotherm constant (J/mol) and R is the gas constant in joules. As illustrated in Fig. 9, B and K_T can be derived from the slopes (B) and intercepts (B ln K_T) of the q_e vs. lnC_e plot.

The results of the applied adsorption models were summarized in Table 1. which demonstrates that the Freundlich model performed better than Langmuir and Temkin with regard of the linear regression correlation coefficient, indicating that the adsorption isotherm is well compatible with the Freundlich equation. The value of 1/n obtained from applying Freundlich equation is less than 1 proves that heterogeneity of adsorption process. The n value, which ranged from 1 to 10, showed favorable adsorption process. The adsorption capacity was only significantly decreased at lower equilibrium concentrations, according to the numerical value of 1/n.[27]

Kinetics of CV dye removal by MPS

Several kinetics approaches were used to further explain the processes of CV adsorption on MPS

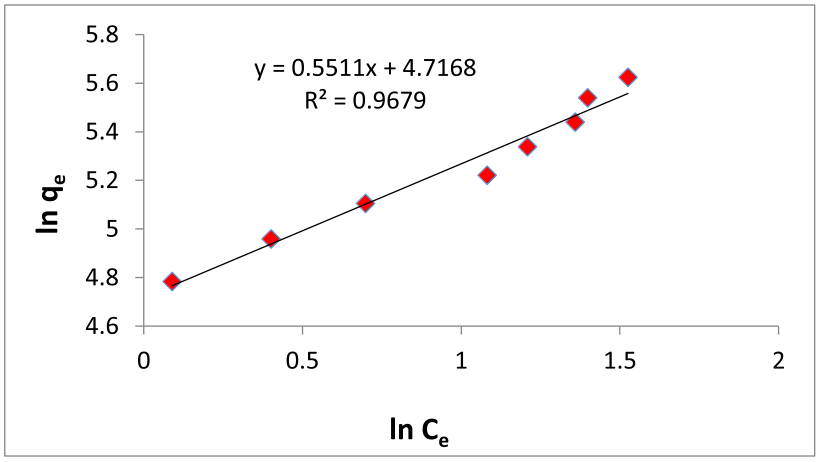

Fig. 8. Linear plot of Freundlich model for CV-MPS adsorption process.

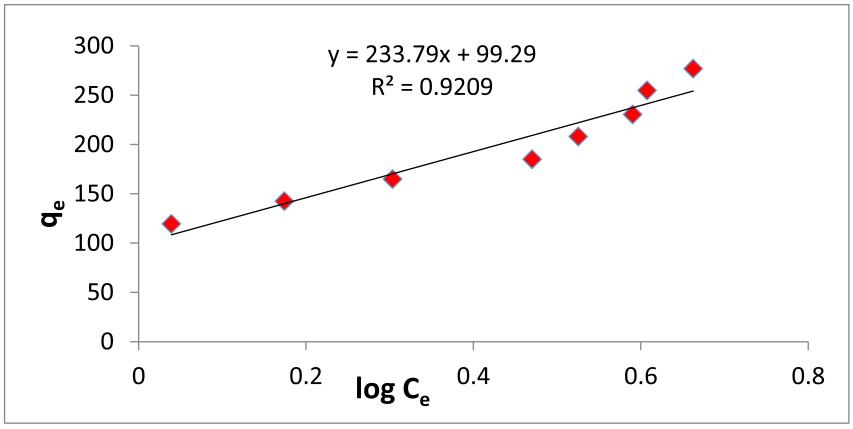

Fig. 9. Linear plot of Temkin model for CV-MPS adsorption process.

Table 1. The estimated constants from the three adsorption isotherms.

Langmuir model			Freundlich model			Temkin model			
R^2	Q_0(mg/g)	K_L(L/mg^{-1})	R^2	1/n	K_f(L/mg^{-1})	R^2	B	b_T(J/mole)	K_T(L/g)
0.8848	434.78	0.306	0.9679	0.551	111.8	0.9209	233.8	10.59	1.53

surfaces. In order investigate the adsorption kinetic behavior of CV (15 mg/l) onto MPS at 298 K, both the Lagergren-first-order equation and pseudo-second-order equation were applied. Considering the resultant values of the linear regression correlation coefficient (R^2), the best-fit model was chosen.

The pseudo-first order kinetic model[28] has the following linear equation form Eq. (5):

$$\log(q_e - q_t) = \log q_e - (k_1/2.303)\, t \quad (5)$$

q_e and q_t represent the quantity of CV adsorbed on the surface of the MPS at equilibrium and at any time respectively, k_1 is the rate constant of the pseudo-first order kinetics (min^{-1}). Estimating q_e and k_1 is often accomplished using the intercept and slope of the plot of log ($q_e - q_t$) vs t, respectively as in Fig. 10.

The linear form Eq. (6) of the pseudo-second order kinetic model[29] is as follows:

$$\frac{t}{q_t} = \frac{1}{k_2 q_e^2} + \left(\frac{1}{q_e}\right) t \quad (6)$$

In this model, k_2 is the rate constant of pseudo-second order kinetics and its unit (g.mg^{-1}.min^{-1}). Fig. 11 illustrates the plot between t/q_t and t which gave linear relation and the intercept and the slope of this linear plot were obtained to determine k_2 and q_e,

In order to assess the diffusion mechanism of adsorption CV dye onto MPS, the Weber and Morris intra-particle diffusion model[30] was used which can

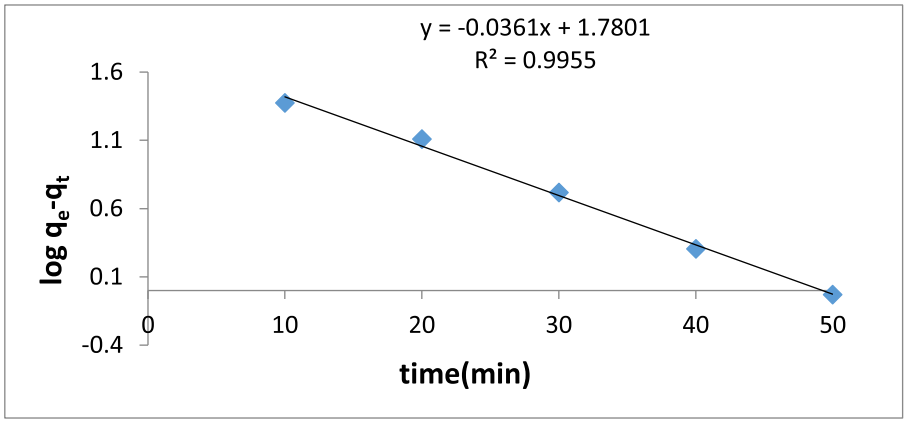

Fig. 10. Plot of Pseudo first order kinetics of adsorption of CV dye at 298 K.

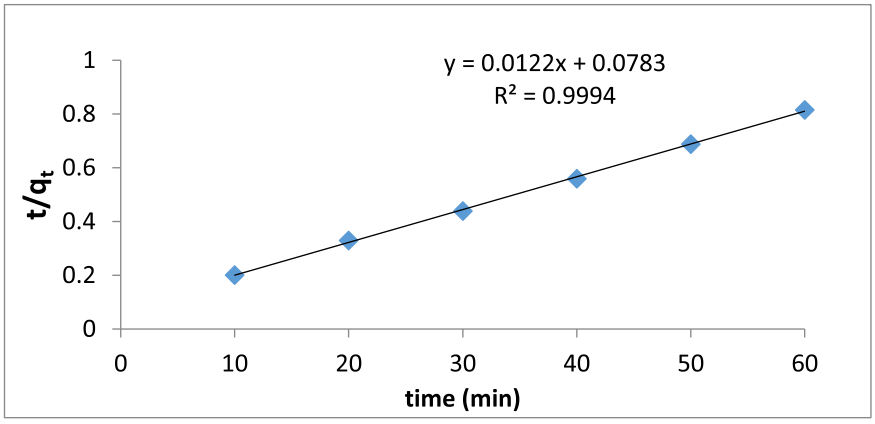

Fig. 11. Plot of Pseudo second order kinetics of adsorption of CV dye at 298 K.

Table 2. Kinetics parameters of Adsorption CV onto MPS.

Pseudo First order			Pseudo Second order			Diffusion model	
R^2	k_1 (min^{-1})	$q_{e\ (mg/g)}$	R^2	k_2(g mg^{-1} min^{-1})	$q_{e\ (mg/g)}$	$k_{dmg/g\ min^{-0.5}}$	R^2
0.9955	0.083	60.27	0.9994	0.0019	81.97	5.2002	0.9125

be presented in the following form Eq. (7):

$$q_t = k_i\, t^{0.5} + C \tag{7}$$

where, k_i (mg g^{-1} $min^{-1/2}$), is the rate constant of intra-particle diffusion and C is the intercept represents the thickness of boundary layer The boundary plays an essential role in film diffusion when adsorbate molecules are transported from the liquid layer to the solid one. The straight line should pass through the origin if intraparticle diffusion is the sole mechanism for adsorption. The slope of the linear relation of the plot between the quantity of CV adsorbed (q_t) against square root of time ($t^{0.5}$), as illustrated in Fig. 12, which can be used to determine the rate constant (k_i).

The parameters and constants were obtained from applying kinetics model as illustrated in Table 2. The second pseudo model has the highest regression coefficient (R^2) of 0.999 indicating the high fitting of adsorption process to this model. Intraparticle diffusion's coefficient R^2 is high, but the value of C shows that the curve, despite being linear, never crossed the origin, confirming that it was not the sole factor affecting rate during adsorption. [31] Therefore, boundary layer control may have been involved in the adsorption of CV onto MPS.

Thermodynamic study

Adsorption studies have been performed to determine the thermodynamic characteristics (free energy change (ΔG°), enthalpy change (ΔH°), and entropy change (ΔS°) at four different temperatures (293–323 K).

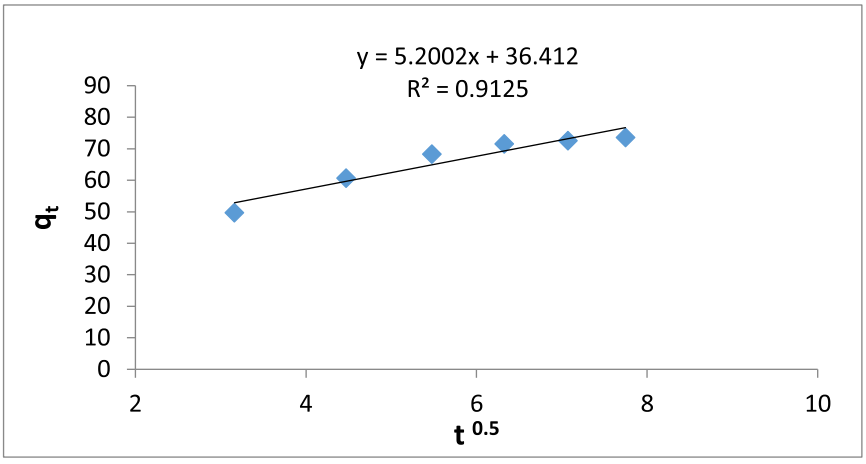

Fig. 12. Plot of intra particle diffusion of adsorption of CV dye at 298 K.

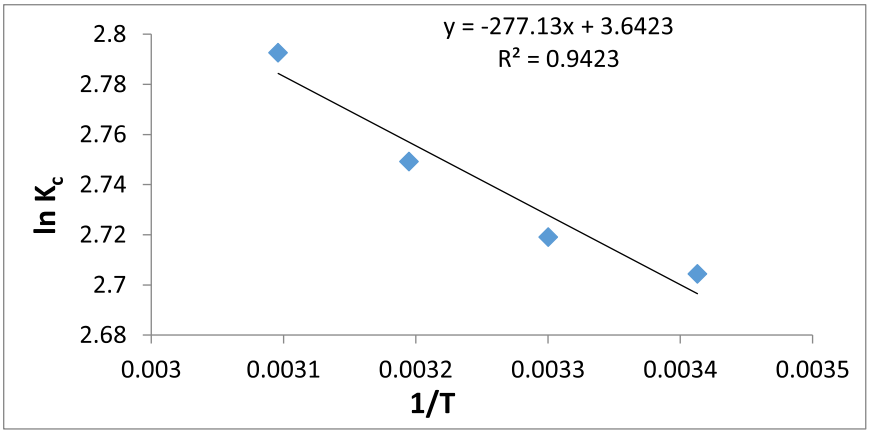

Fig. 13. Van't Hoff plot of adsorption CV onto MPS at (293–323) K.

The thermodynamic functions in Eqs. (8) and (9) was calculated as follow:[32]

$$\Delta G^{\circ} = -RT \ln K_L \quad (8)$$

$$\ln K_c = \frac{\Delta S^{\circ}}{R} - \frac{\Delta H^{\circ}}{RT} \quad (9)$$

R is gas constant (J/mol K), T the absolute temperature (K) and K_L is the equilibrium constant (L/g). The values of (ΔH°) and (ΔS°) were calculated using the van't Hoff plots of ln(K_c) versus 1/T. Fig. 13 depicts the plotting of this relationship, and Table 3. provides the thermodynamic parameters estimated at various studied temperatures.

The negative ΔG° values demonstrate the spontaneous character of the adsorption process and show that lower temperatures are preferable for adsorption. The positive value of (ΔH°) (2.304 kJ/mol) confirmed the adsorption reaction is endothermic in nature and it is less than (40 kJ/mol) which proves that adsorption of CV dye onto MPS was a physical process.[33] The positive value (ΔS°) points to an increase in randomness distribution of CV dye molecules on the solid phase (MPS) and a consequent its concentration drops in adsorbate at the solid-solution interface.[34]

Table 3. Thermodynamic parameters of adsorption CV onto MPS at (293–323) K.

Temp.(K)	ΔG° (kJ/mol)	ΔH° (kJ/mol)	ΔS° (J/K.mol)
293	–6.59	2.30	30.28
303	–6.85		
313	–7.15		
323	–7.50		

Conclusion

High surface area equals to 778. m^2/g of MPS was obtained by hydrothermal synthesis method using a low cost precursor sodium silicate. The prepared sample was examined as adsorbent surface for crystal

violet dye and was proven that it was efficient surface due to high value of quantity adsorbed of CV dye on it. The Freundlich model gave high comply with adsorption parameters. The kinetics of adsorption reveals that pseudo second order is g fitness model to the adsorption of CV onto MPS. Low temperatures are preferable to carry the adsorption process was concluded due to the thermodynamic parameters represented by increasing the negative value of free energy with increasing in temperature.

Authors' declaration

- Conflicts of Interest: None.
- We hereby confirm that all the figures and tables in the manuscript are ours. Furthermore, any figures and images, which are not ours, have been included with the necessary permission for republication, which is attached to the manuscript.
- No animal studies are present in the manuscript.
- No human studies are present in the manuscript.
- Ethical Clearance: The project was approved by the local ethical committee at University of Baghdad.

Authors contribution statements

I. H. A. and E. A. H. designed the study. A. H. H. and E. A. H. performed the experiments. I. H. A. and S. A. D. analyzed the data and wrote the paper with input from all authors.

References

1. Hussein EA, Kareem SH. Magnetic mesoporous silica material (Fe_3O_4@$MSiO_2$) as adsorbent and delivery system for ciprofloxacin drug. IOP Conf Ser: Mater Sci Eng. 2020;871:012020. https://doi.org/10.1088/1757-899x/871/1/012020.
2. Feng Q, Wei F, Chen Z, Huang Z, Hu H, Liang F, *et al.* Mesoporous silica-based catalysts for photocatalytic CO_2 reduction. Microporous Mesoporous Mater. 2024;366:112947. https://doi.org/10.1016/j.micromeso.2023.112947.
3. Fu Y, Li Q, Sun X, Li X, Cheng L, Yang J, *et al.* Synthesis of mixed-mode based functionalized mesoporous silica through raft polymerization and its application for dye adsorption. Microporous Mesoporous Mater. 2023;350:112462. https://doi.org/10.1016/j.micromeso.2023.112462.
4. Abdullah, K M, Shah NA, Chung JD. A review on thermochemical seasonal solar energy storage materials and modeling methods. Int J Air-Cond Ref. 2024;32(1):1–26. https://doi.org/10.1007/s44189-023-00044-6.
5. Gu L, Zhang A, Hou K, Dai C, Zhang S, Liu M, *et al.* One-pot hydrothermal synthesis of mesoporous silica nanoparticles using formaldehyde as growth suppressant. Microporous Mesoporous Mater. 2012;152(1 Apr):9–15. https://doi.org/10.1016/j.micromeso.2011.11.047.
6. Willinger M, Felhofer M, Reimhult E, Zirbs R. Method for high-yield hydrothermal growth of silica shells on nanoparticles. Materials (Basel). 2021;14(21):6646. https://doi.org/10.3390/ma14216646.
7. Ashour MM, Mabrouk M, Soliman IE, Beherei HH, Tohamy KM. Mesoporous silica nanoparticles prepared by different methods for biomedical applications: Comparative study. IET Nanobiotechnol. 2021;15(3):291–300. https://doi.org/10.1049/nbt2.12023.
8. Akhter F, Rao AA, Abbasi MN, Wahocho SA, Mallah MA, Anees-ur-Rehman H, *et al.* Comprehensive review of synthesis, applications and future prospects for silica nanoparticles (SNPs). Silicon. 2022;14(14):8295–310. https://doi.org/10.1007/s12633-021-01611-5.
9. Kresge CT, Leonowicz ME, Roth WJ, Vartuli JC, Beck JS. Ordered mesoporous molecular sieves synthesized by a liquid-crystal template mechanism. Nature. 1992 Oct;359(6397):710–712. https://doi.org/10.1038/359710a0.
10. Zhao D, Feng J, Huo Q, Melosh N, Fredrickson GH, Chmelka BF, *et al.* Triblock copolymer syntheses of mesoporous silica with periodic 50 to 300 angstrom pores. Science. 1998;279(5350):548–552. https://doi.org/10.1126/science.279.5350.548.
11. Che S, Garcia-Bennett AE, Yokoi T, Sakamoto K, Kunieda H, Terasaki O, *et al.* A novel anionic surfactant templating route for synthesizing mesoporous silica with unique structure. Nat Mater. 2003;2(12):801–805. https://doi.org/10.1038/nmat1022.
12. Heidari A, Younesi H, Mehraban Z. Removal of ni(ii), CD(II), and pb(ii) from a ternary aqueous solution by amino functionalized mesoporous and nano mesoporous silica. Chem Eng J. 2009;153(1-3):70–79. https://doi.org/10.1016/j.cej.2009.06.016.
13. Ali IH. Removal of congo red dye from aqueous solution using eco-friendly adsorbent of Nanosilica. Baghdad Sci J. 2021;18(2):366–373. https://doi.org/10.21123/bsj.2021.18.2.0366.
14. Slama HB, Chenari Bouket A, Pourhassan Z, Alenezi FN, Silini A, Cherif-Silini H, *et al.* Diversity of synthetic dyes from textile industries, discharge impacts and treatment methods. Appl Sci. 2021;11(14):6255. https://doi.org/10.3390/app11146255.
15. Mousa SA. A comparative study of the adsorption of crystal violet dye from aqueous solution on rice husk and charcoal. Baghdad Sci J. 2020;17(1):0295. https://doi.org/10.21123/bsj.2020.17.1(suppl.).0295.
16. Nizam NU, Hanafiah MM, Mahmoudi E, Halim AA, Mohammad AW. The removal of anionic and cationic dyes from an aqueous solution using biomass-based activated carbon. Sci Rep. 2021;11(8623). https://doi.org/10.1038/s41598-021-88084-z.
17. Chen Y-S, Ooi CW, Show PL, Hoe BC, Chai WS, Chiu C-Y, *et al.* Removal of ionic dyes by nanofiber membrane functionalized with chitosan and egg white proteins: Membrane preparation and adsorption efficiency. Membranes. 2022 Jan 1;12(1):63. https://doi.org/10.3390/membranes12010063.
18. Jia J, Wu H, Xu L, Dong F, Jia Y, Liu X. Removal of acidic organic ionic dyes from water by electrospinning a polyacrylonitrile composite mil101(fe)-nh2 nanofiber membrane. Molecules. 2022 Mar 21;27(6):2035. https://doi.org/10.3390/molecules27062035.

19. Tolkou AK, Mitropoulos AC, Kyzas GZ. Removal of anthraquinone dye from wastewaters by hybrid modified activated carbons. Environ Sci Pollut Res Int. 2023;30(29): 73688–73701. https://doi.org/10.1007/s11356-023-27550-9.
20. Homagai PL, Poudel R, Poudel S, Bhattarai A. Adsorption and removal of crystal violet dye from aqueous solution by modified rice husk. Heliyon. 2022 Apr 7;8(4):e09261. https://doi.org/10.1016/j.heliyon.2022.e09261.
21. Sing KS. Reporting physisorption data for gas/solid systems with special reference to the determination of surface area and porosity (provisional). Pure Appl Chem. 1982;54(11):2201–2218. https://doi.org/10.1351/pac198254112201.
22. Dleam EA, Kareem SH. Mesoporous silica nanoparticles as a system for ciprofloxacin drug delivery; kinetic of adsorption and releasing. Baghdad Sci J. 2021;18(2):0357. https://doi.org/10.21123/bsj.2021.18.2.0357.
23. Samadi-Maybodi A, Vahid A. Synthesis of mesoporous silica nanoparticles by means of a hydrogel. Int Nano Lett. 2013;3(39):1–3. https://doi.org/10.1186/2228-5326-3-39.
24. Gebreslassie YT. Equilibrium, kinetics, and thermodynamic studies of malachite green adsorption onto fig (*ficus cartia*) leaves. J Anal Methods Chem. 2020 Mar 4;7384675:1–11. https://doi.org/10.1155/2020/7384675.
25. Lan D, Zhu H, Zhang J, Li S, Chen Q, Wang C, *et al.* Adsorptive removal of organic dyes via porous materials for wastewater treatment in recent decades: A review on species, mechanisms and perspectives. Chemosphere. 2022 Apr;293: 133464. https://doi.org/10.1016/j.chemosphere.2021.133464.
26. Edet UA, Ifelebuegu AO. Kinetics, isotherms, and thermodynamic modeling of the adsorption of phosphates from model wastewater using recycled brick waste. Processes. 2020;8(6):665. https://doi.org/10.3390/pr8060665.
27. Pantanit S, Injongkol Y, Jungsuttiwong S, Bremner JB, Chairat M. Adsorption kinetic and thermodynamic studies of the dyeing process of pineapple leaf fibre with berberine dye and modeling of associated interactions. Arab J Basic App Sci. 2023;30(1):354–67. https://doi.org/10.1080/25765299.2023.2218199.
28. Muslim M, Ali A, Kamaal S, Ahmad M, Jane Alam M, Rahman QI, *et al.* Efficient adsorption and facile photocatalytic degradation of organic dyes over H-bonded proton-transfer complex: An experimental and theoretical approach. J Mol Liq. 2022;347(1 Feb):117951. https://doi.org/10.1016/j.molliq.2021.117951.
29. Hasani N, Selimi T, Mele A, Thaçi V, Halili J, Berisha A, *et al.* Theoretical, equilibrium, kinetics and thermodynamic investigations of methylene blue adsorption onto lignite coal. Molecules. 2022 Mar 12;27(6):1856. https://doi.org/10.3390/molecules27061856.
30. Wang W, Maimaiti A, Shi H, Wu R, Wang R, Li Z, *et al.* Adsorption behavior and mechanism of emerging perfluoro-2-propoxypropanoic acid (genx) on activated carbons and resins. J Chem Eng. 2019;364:132–138. https://doi.org/10.1016/j.cej.2019.01.153.
31. Wang J, Guo X. Rethinking of the intraparticle diffusion adsorption kinetics model: Interpretation, solving methods and applications. Chemosphere. 2022 Dec;309(Pt2):136732. https://doi.org/10.1016/j.chemosphere.2022.136732.
32. Nogueira DA, Zanela TM, Machado MV, Almeida CA, Marangoni R. Adsorption process of methyl orange dye onto zinc hydroxide nitrate: Kinetic and thermodynamic studies. Colorants 2023;2(3):565–577. https://doi.org/10.3390/colorants2030028.
33. Bai C, Wang L, Zhu Z. Adsorption of cr(iii) and pb(ii) by graphene oxide/alginate hydrogel membrane: Characterization, adsorption kinetics, isotherm and thermodynamics studies. Int J Biol Macromol. 2020 Mar 15;147:898–910. https://doi.org/10.1016/j.ijbiomac.2019.09.249.
34. Parimelazhagan V, Natarajan K, Shanbhag S, Madivada S, Kumar HS. Effective adsorptive removal of coomassie violet dye from aqueous solutions using green synthesized zinc hydroxide nanoparticles prepared from calotropis gigantea leaf extract. ChemEngineering. 2023;7(2):31. https://doi.org/10.3390/chemengineering7020031.

التحضير الهيدروحراري لسيليكا متوسطة المسام ذات مساحة سطحية عالية كمادة مازة فعالة لازالة صبغة الكرستال البفسجية من محاليلها المائية

انعام حسين علي، اميرة حسن حمد، ايناس عبد الحسين، سعدية احمد ظاهر

قسم الكيمياء، كلية العلوم للبنات، جامعة بغداد، بغداد، العراق.

المستخلص

في هذه الدراسة ، تم تحضير نموذج من سيليكا متوسطة المسام ذات مساحة سطحية عالية بطريقة التحضير الهيدروحراري. وللتحقق من خواص المادة المحضرة تم تحليل النموذج باستخدام عدة تقنيات مثل امتزاز- تحرير النايتروجين، مجهر القوة الماسحة، تشتت اشعة X و مجهر القوة الذرية. من اجل تقييم كفاءة السيليكا المحضرة تم اجراء دراسة امتزاز على سطح السيليكا لإزالة صبغة الكرستال البنفسجية من المحاليل المائية. تمت الدراسة في ظروف مختلفة من التركيز الابتدائي للصبغة وكمية السيليكا بالاضافة مدى درجات حرارة من (293- 323) كلفن. تم تطبيق ثلاث معادلات امتزاز وهي لانكماير، فرندلج وتمكن على النتائج المستحصلة والتي اعطت تطابقا عاليا مع معادلة فرندلج. تم دراسة حركية الامتزاز باستخدام معادلتي الدرجة الاولى الكاذبة والدرجة الثانية الكاذبة، إضافة الى معادلة الانتشار بين الدقائق. ولقد تبين ان ازالة صبغة الكرستال البنفسجية على سطح السيليكا هي من الدرجة الثانية الزائفة وان خطوة الانتشار لم تكن الخطوة الوحيدة المحددة لعملية الامتزاز لان معادلة الانتشار بين الدقائق الخطية لم تمر بنقطة الاصل. الدراسة الدينمية الحرارية لعملية الامتزاز بينت ان طبيعة التفاعل تلقائي وماص للحرارة.

الكلمات المفتاحية: الكرستال البنفسجية، مساحة سطحية عالية، هيدروحراري، سيليكا متوسطة المسام، سيليكات الصوديوم.